CHAPTER 6 FATIGUE PROPERTIES OF EMULSION TREATED MATERIALS

6.1 INTRODUCTION

Most materials bound by cement and/or bitumen show fatigue resistance properties that will resist the formation of tensile failure areas (cracks) when subjected to tensile stresses or strains. Fatigue has been defined as "*the process of progressive localised permanent structural change occurring in a material subjected to conditions which produce fluctuating stresses and strains at some point or points and which may culminate in cracks or complete fracture after a sufficient number of fluctuations*" (ASTM: 1964). Fatigue will therefore start when the material is repeatedly subjected to a load that induces a tensile strain in the material. Early in their life, as a component in a pavement structure, treated materials act similarly to a loaded beam. Tensile strains develop mainly at the bottom of these layers and will initiate the breaking up of the bonds formed by cement and bitumen. This will lead subsequently to the formation of cracks, which may in some cases be of microscopic size.

Cracking in pure cementitious layers can be divided into non-traffic associated cracking and traffic associated cracking. The non-traffic associated cracking involves cracking due to environmental conditions such as temperature and moisture content. Research on non-traffic associated cracking in emulsion treated layers is limited, but the performance from emulsion treated layers with cement in the field has proved that there is less non-traffic associated cracking than in pure cement treated layers.

Cracking in bituminous bases and surfacings, usually occurs due to the combined effect of traffic loading and ageing of the bituminous binder.

The scope of this chapter includes the analysis of the fatigue properties observed of the emulsion treated material tested. A failure criterion for the effective fatigue life is also developed for the use in structural design.

6.2 THE END OF THE FATIGUE LIFE

The fatigue life of a treated pavement material is normally characterised by a high modulus of elasticity, low elastic deflections and virtually no permanent deformation. The end of the fatigue life resulted in a non-linear behaviour because of the non-homogeneity from the presence of cracks, a reduced modulus of elasticity, increased elastic deflection and a decrease in the resistance to permanent deformation. The initiation of cracks in a layer will lead to a reduction in the stiffness that will lead to a further reduction as the cracks progress through the layer. The end of the fatigue life of a bound pavement layer will therefore consists of two

phases, namely the crack initiation phase and crack progression phase. The progression of cracks through the layer may not necessarily be linear through the layer and the speed of crack propagation may vary as the balance and stress state of the pavement vary.

The effective fatigue life is defined as the stage in the life of the layer where the crack (whatever its size) progresses through the layer and the effective stiffness of the layer is reduced to similar values as found in granular or unbound layers.

The effective stiffness of the ferricrete at Vereeniging seems to converge to a terminal stiffness value of around 500 MPa after a number of load repetitions. The point at which the effective stiffness reaches a value of 500 MPa, is approximately 25% of the initial stiffness in this case, and is assumed to be the end of the fatigue life phase of the ferricrete material. The layer is then in a reduced stiffness phase equivalent to a granular layer although the layer may still be largely intact and only broken down in large blocks.

6.3 TENSILE STRAIN ANALYSIS

Horizontal tensile strains at the bottom of the layer were calculated at various load repetitions during the HVS tests. The strains were calculated using a linear elastic multilayer software package with stiffnesses as backcalculated in Chapter 5. Figure 6.1 contains a plot from the analysis on a linear-log scale.

The horizontal tensile strain at the bottom of the layer showed a relatively stable increase in strain up to a point where it starts to oscillate. This was consistent at all the test sections and MDD's where no load history was present. A closer look at the elastic deflections, as well as the backcalculated stiffness, revealed that both these parameters entered an unstable phase although it is not easily visible. The elastic deflection decreased immediately after this point, while the resilient modulus increased. The point is preceded by a sharper increase in tensile strain as indicated in Figure 6.1.

This behaviour indicated that there were some changes in the behaviour of the pavement at this point, which is caused by the development of cracks in the close vicinity of the MDD module at the bottom of the emulsion treated layer. After the formation of the cracks there was a redistribution of the stresses around the MDD module at the bottom of the layer that lead to the reduction in the elastic deflection. The horizontal strains at the bottom of the layer were then concentrated around the cracks as shown in Figure 6.2.

Figure 6.3 presents the maximum horizontal tensile strain before crack initiation, at various positions within the layer. The tensile strains were determined using a multi-layer linear elastic software program, and it confirms that the maximum horizontal strain for the pavement structure under consideration is at the bottom of the layer.

The life to crack initiation for each of the HVS tests is summarised in Table 6.1 and Figure 6.4 presents a transfer function to determine the life to crack initiation.

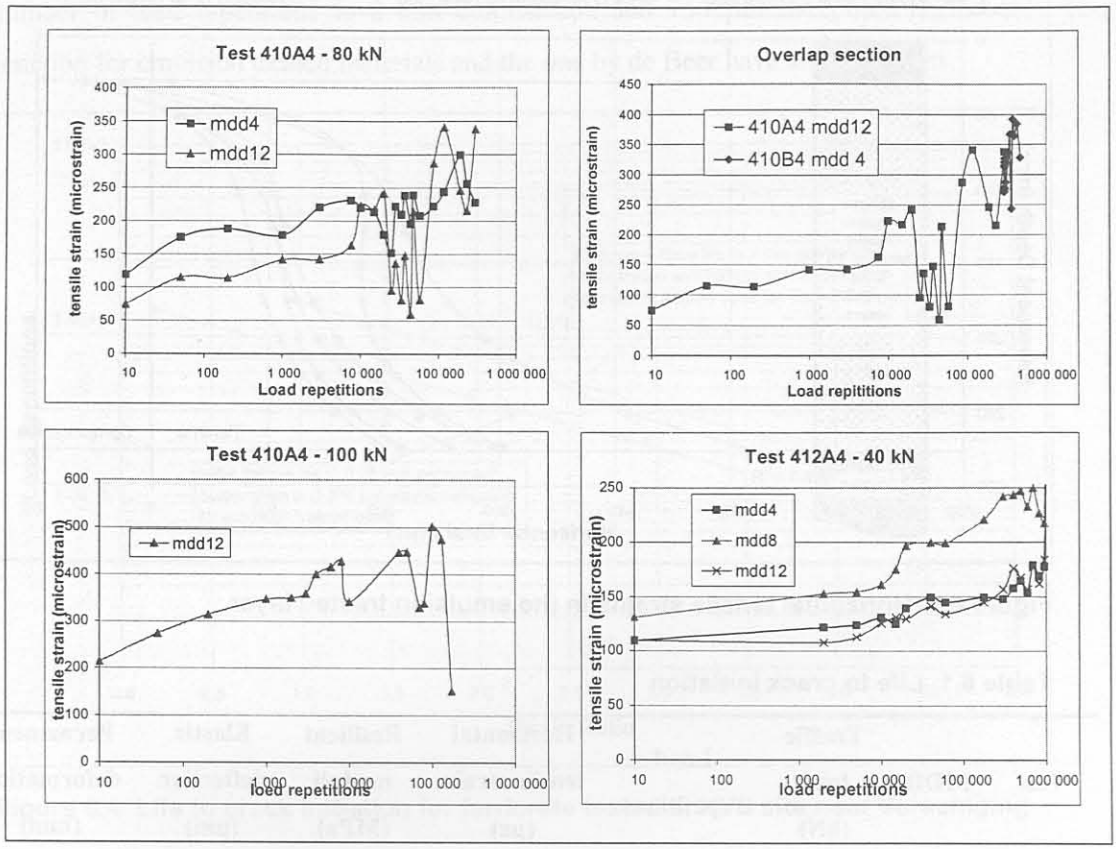

Figure 6.1 Tensile strain analysis

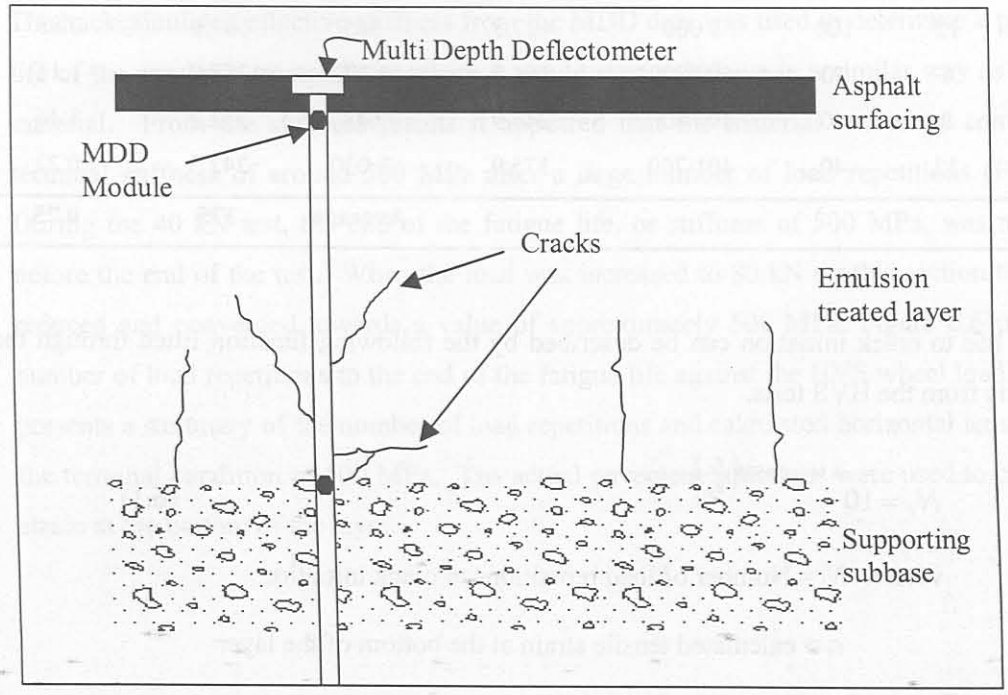

Figure 6.2 Schematic illustration of the initiation of cracks at the MDD at bottom of the layer

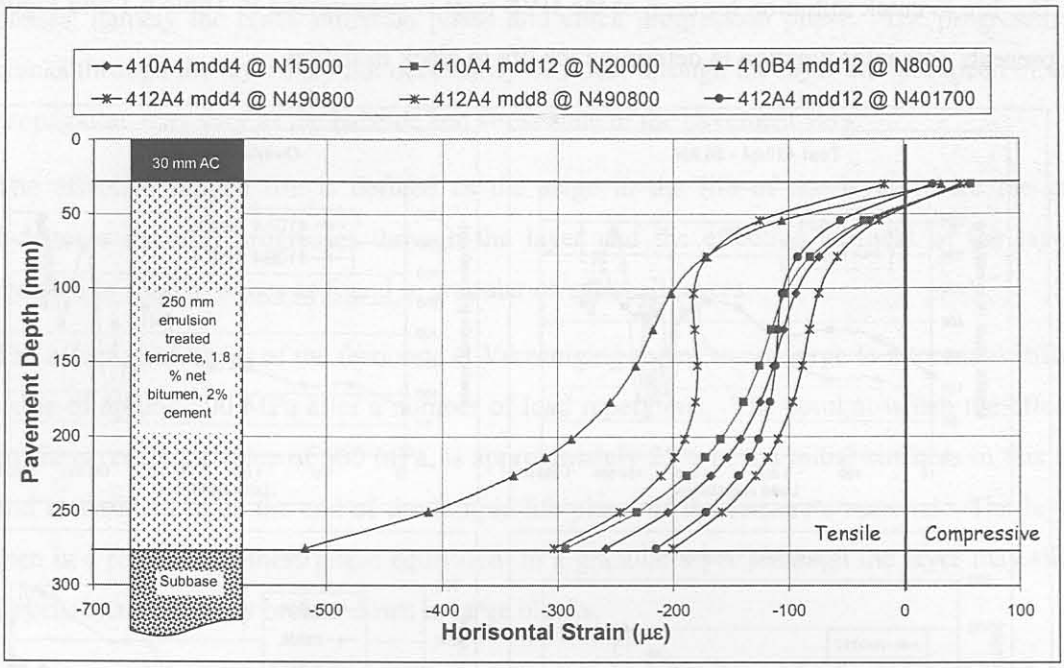

Figure 6.3 Horizontal tensile strains in the emulsion treated layer.

Table 6.1 Life to crack initiation

Test	MDD	Traffic load (kN)	Load repetitions	Horizontal tensile strain (με)	Resilient moduli (MPa)	Elastic deflection (μm)	Permanent deformation (mm)
410A4	4	80	15 000	213.5	1 042	361.4	0.53
410A4	12	80	20 000	241.6	969	391.3	0.28
410B4	12	100	8 000	427.5	565	667.0	0.85
412A4	4	40	490 800	164.8	1 302	258.0	1.11
412A4	8	40	490 800	246.9	648	332.2	1.46
412A4	12	40	401 700	175.9	1 030	242.5	0.22
					Average	**375**	**0.75**

The life to crack initiation can be described by the following function fitted through the data points from the HVS tests.

$$N_i = 10^{6.344-0.8573\left(\frac{\varepsilon_t}{\varepsilon_b}\right)} \qquad (6.1)$$

where: N_i = Number of load repetitions to crack initiation

ε_t = calculated tensile strain at the bottom of the layer

ε_b = strain at break

This equation is similar to the one developed by de Beer (1989) for crack initiation in lightly cemented materials. De Beer defined crack initiation in lightly cemented materials as the number of load repetitions to 2 mm deformation and 750 μm maximum deflection. The function for emulsion treated materials and the one by de Beer have similar slopes.

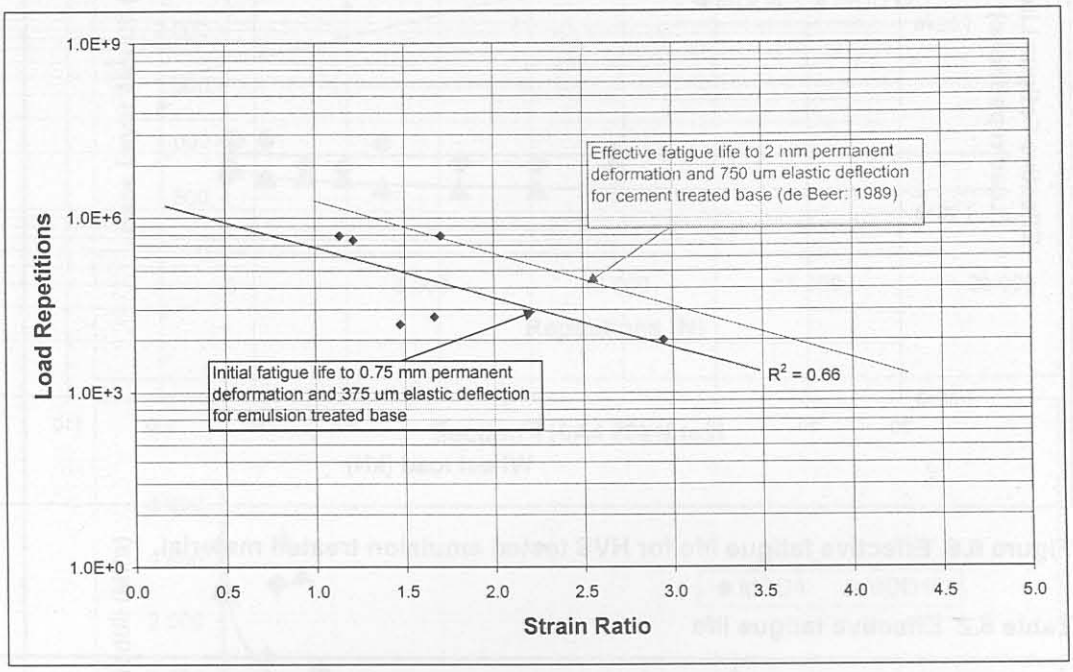

Figure 6.4 Life to crack initiation for ferricrete tested at HVS site near Vereeniging

6.4 THE EFFECTIVE FATIGUE LIFE OF EMULSION TREATED MATERIALS

The backcalculated effective stiffness from the MDD data was used to determine a point in the life of the emulsion treated layer where it would start to behave in a similar way as a granular material. From the stiffness results it appeared that the material tended to converge to a terminal stiffness of around 500 MPa after a large number of load repetitions (Figure 6.5). During the 40 kN test, the end of the fatigue life, or stiffness of 500 MPa, was not reached before the end of the test. When the load was increased to 80 kN on this section the stiffness reduced and converged towards a value of approximately 500 MPa. Figure 6.6 presents the number of load repetitions to the end of the fatigue life against the HVS wheel load. Table 6.2 presents a summary of the number of load repetitions and calculated horizontal tensile strain at the terminal condition of 500 MPa. The actual pavement structures were used to calculate the strain at the bottom of the layer.

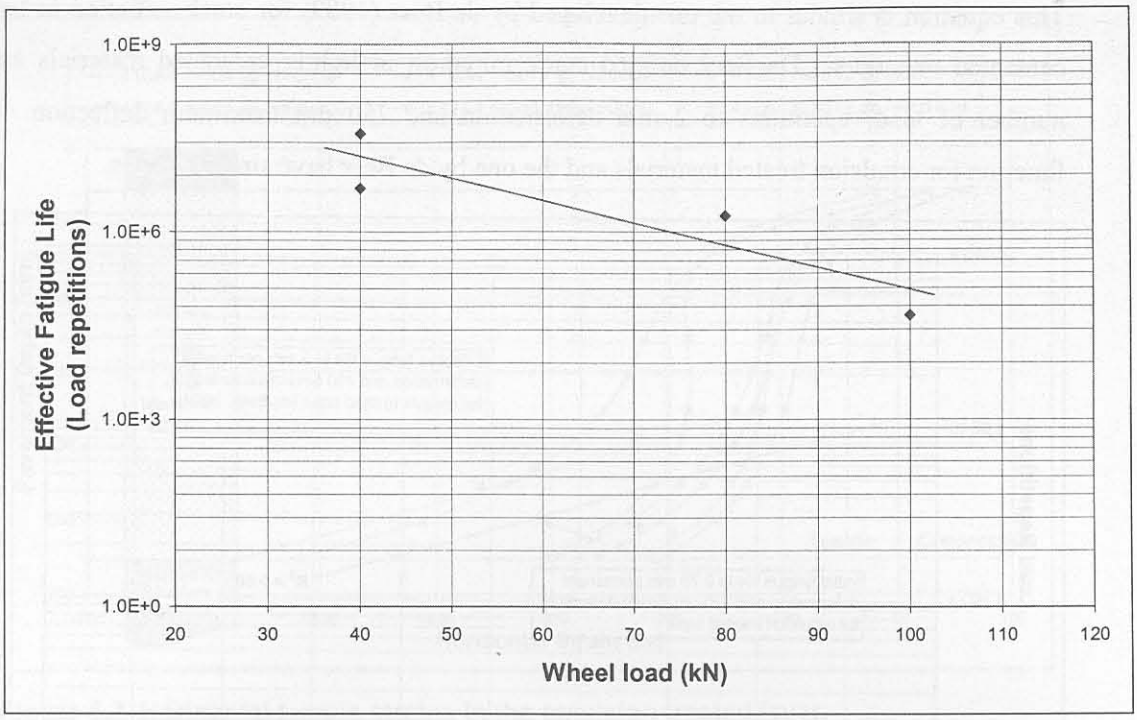

Figure 6.6 Effective fatigue life for HVS tested emulsion treated material.

Table 6.2 Effective fatigue life

Test	MDD	Load	ε_t	ε_b	Strain ratio ($\varepsilon_t/\varepsilon_b$)	N
410A4*	4	80	270.0	145	2.048	$3.53 * 10^6$
410A4	12	80	301.3	145	2.078	$1.8 *10^6$
410B4	12	100	437.0	145	3.013	$45.4*10^3$
412A4	4	40	133.2	145	0.918	$3.2 *10^9$
412A4	8	40	135.3	145	0.933	$5.0 * 10^6$
412A4	12	40	119.6	145	0.825	$37.2 * 10^6$

A curve was fitted through the data above which included various strain at break values. The effective fatigue life for the material tested, can be expressed as follows:

$$N_{eff} = 10^{8.5066-1.2774\left(\frac{\varepsilon_t}{\varepsilon_b}\right)} \quad (6.2)$$

where: N_{eff} = Effective fatigue life

ε_t = calculated tensile strain at the bottom of the layer

ε_b = strain at break

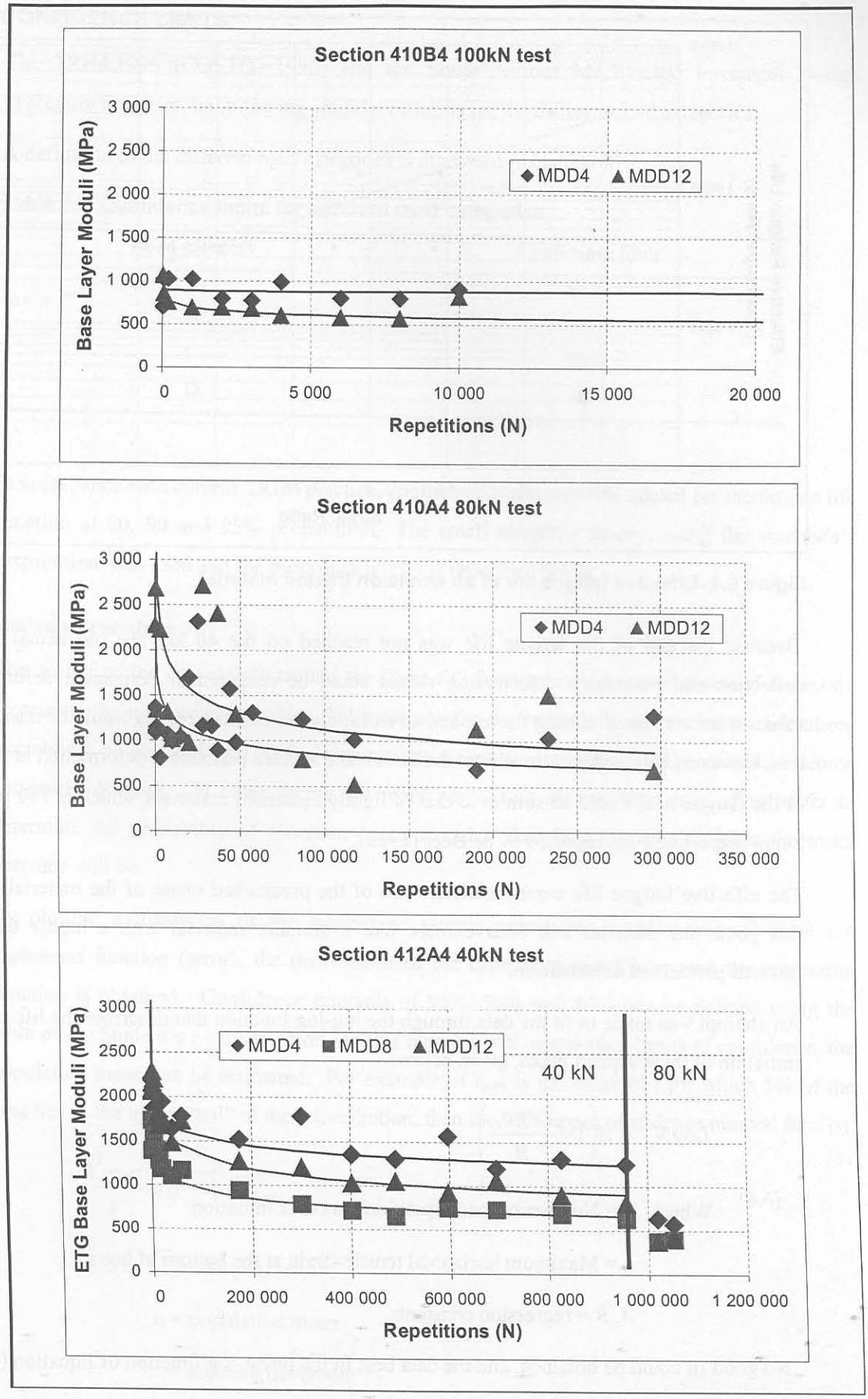

Figure 6.5 Reduction in stiffness with increase in load repetitions on HVS test sections

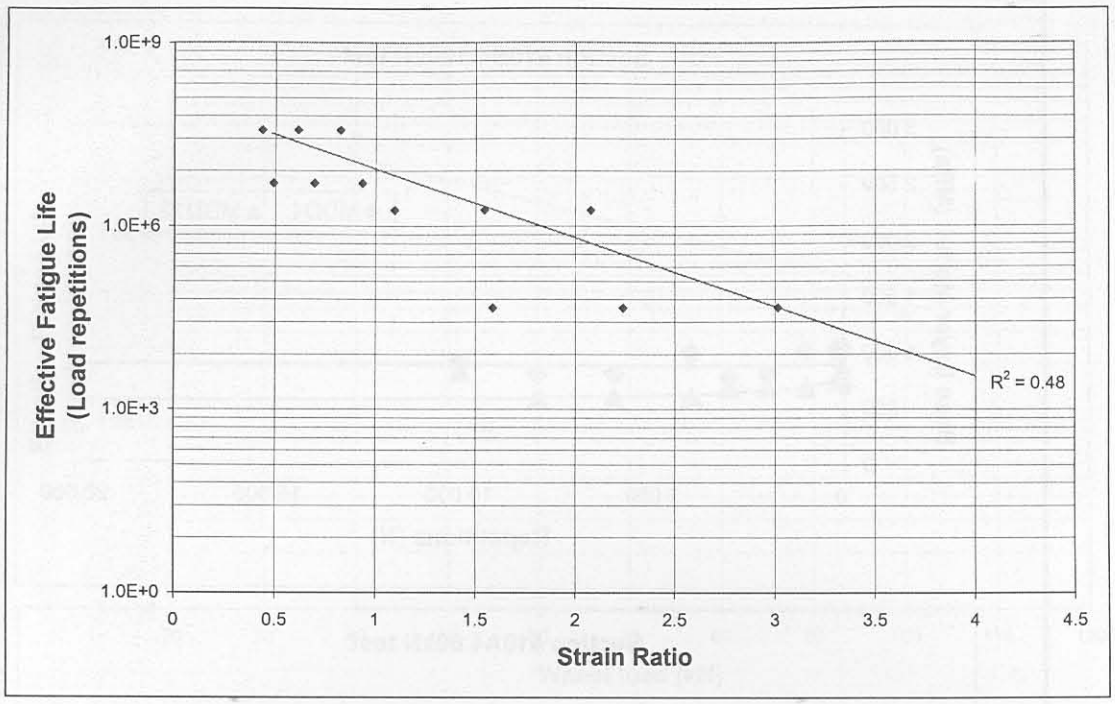

Figure 6.6 Effective fatigue life of an emulsion treated material

Because the end of the fatigue life was not reached on the 40 kN test, no actual elastic deflection and permanent deformation values could be determined. Permanent deformation values were very small during the test and an extrapolation of these results would be inaccurate. It is, however, believed that the elastic deflection and surface permanent deformation at the end of the fatigue life, would be similar to that of lightly cemented materials, which is 750 μm and 2 mm respectively, as reported by de Beer (1989).

The effective fatigue life would mark the end of the precracked phase of the material. After this point, the material will behave more like a granular material with a higher tendency towards permanent deformation.

An attempt was made to fit the data through the log-log function that describes the life to crack initiation of thick asphalt bases, given below.

$$LogN_f = A\left(1 - \frac{Log\varepsilon_t}{B}\right) \tag{6.3}$$

Where: N_f= Number of load repetitions to crack initiation

ε_t = Maximum horizontal tensile strain at the bottom of layer

A, B = regression constants

No good fit could be obtained, and the data best fit the linear-log function of Equation (6.2).

6.5 CONFIDENCE LIMITS

The TRH4:1996 (COLTO: 1996) and the South African Mechanistic Pavement Design Procedure proposes the following confidence limits for the different road categories.

A definition of the different road categories is discussed in chapter 8.

Table 6.3 Confidence limits for different road categories

Road category	Confidence limit
A	95%
B	90%
C	80%
D	50%

In accordance with current TRH4 practice, confidence limits were calculated for the fatigue life function at 80, 90 and 95% probability. The small sampling theory, using the student's t distribution, was used and the procedure briefly is described below.

6.5.1 Analysis Procedure

The scatter of the data points around the "best fit" function is to be expected, and indirectly represents the number of variables that influence the dependant variable under consideration. Variability of material and design parameters makes the prediction of a specific outcome extremely difficult. In cases where the input parameters are variable, it is often better to determine the probability of a certain outcome rather than to try to predict what the exact outcome will be.

By plotting a histogram of the number of sample points per distance interval from the regression function (error), the distribution of the dependant variable around the regression function is obtained. Confidence intervals of 95%, 90% and 80% can be defined using the table of the Student's t – distribution. In this manner, within specified limits of confidence, the population mean can be estimated. For example, if $t_{0.95}$ is the value of t for which 5% of the area lies in the upper "tail" of the t distribution, then the 95% upper confidence interval for t is:

$$\frac{\overline{X}-\mu}{s}\sqrt{N-1} < t_{0.95} \qquad (6.4)$$

where: $\overline{X}$ = sample mean

μ = population mean

s = standard deviation

N = Sample size

From which we can see that μ is estimated to lie in the interval:

$$\mu < \overline{X} + t_{0.95} \frac{s}{\sqrt{N-1}} \tag{6.5}$$

with 95% confidence (i.e. probability of 0.95). It therefore means that there is a 95% confidence that the distance interval from the regression function, or "error", will be lower than determined in Equation 6.5.

In general, we can represent the upper confidence limit for population means by:

$$\overline{X} + t_c \frac{s}{\sqrt{N-1}} \tag{6.6}$$

where the value t_c, called the *critical value* or *confidence coefficients*, depends on the level of confidence desired and the sample size. They can be read of the tables for the student's t distribution.

The transfer function sample data consists of small samples seldom including repeat tests. It was therefor necessary to make the assumption that there was no "lack of fit" error in the regression functions for the transfer function data and that the variation of the dependant variable around the regression function was not influenced by the value of the independent variable. Under this assumption the confidence limits for the dependant variable will be equal distances from the regression function regardless of the value of the independent variable. A second function representing the confidence limit may therefor be drawn equal distances from the regression function. This is illustrated in Figure 6.7.

6.5.2 Transfer functions for fatigue life for different road categories

Applying the confidence intervals as described above, the transfer functions for fatigue life for the different road categories can be presented as follows:

Category A: $$N_{f_A} = 10^{7.9183 - 1.2775\left(\frac{\varepsilon_t}{\varepsilon_b}\right)} \tag{6.7a}$$

Category B: $$N_{f_B} = 10^{8.0331 - 1.2775\left(\frac{\varepsilon_t}{\varepsilon_b}\right)} \tag{6.7b}$$

Category C: $$N_{f_C} = 10^{8.1747 - 1.2775\left(\frac{\varepsilon_t}{\varepsilon_b}\right)} \tag{6.7c}$$

Category D: $$N_{f_D} = 10^{8.5066 - 1.2775\left(\frac{\varepsilon_t}{\varepsilon_b}\right)} \tag{6.7d}$$

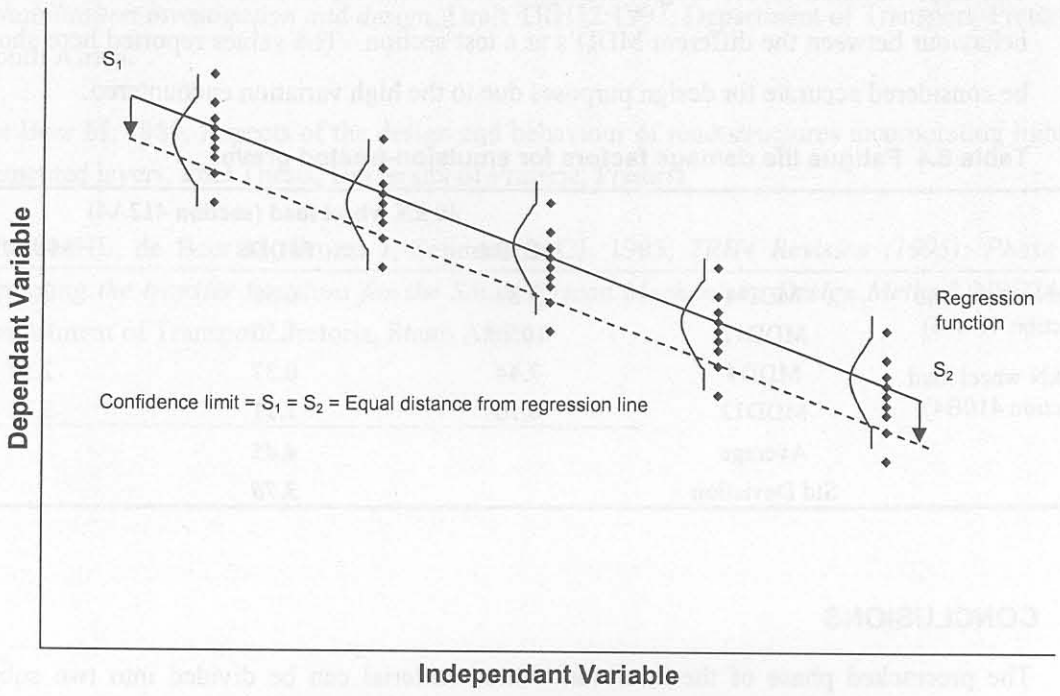

Figure 6.7 Confidence limits represented by a second function drawn parallel to the regression function

6.6 FATIGUE LIFE DAMAGE FACTOR

The HVS data can also be used to determine the load sensitivity and damage factors for a material. The damage factor, n, is used in Equation 6.8 to determine the damage caused by a particular wheel load relative to the damage caused by a standard wheel load.

$$\left(\frac{N_x}{N_{std}}\right)=\left(\frac{P_x}{P_{std}}\right)^n \qquad (6.8)$$

where: N_x = load repetitions at wheel load

N_{std} = load repetitions at standard wheel load

P_x = wheel load

P_{std} = standard wheel load

n = damage factor

Damage factors were calculated by relating a certain defect under a 80 kN and 100 kN wheel load, to that under a 40 kN wheel load. The 40 kN HVS wheel load is equivalent to a 80 kN standard axle load. The damage factors calculated for fatigue life are presented in Table 6.3.

The high variation in the fatigue damage factor is the result of the difference in the fatigue behaviour between the different MDD's at a test section. The values reported here should not be considered accurate for design purposes due to the high variation encountered.

Table 6.4 Fatigue life damage factors for emulsion-treated gravel

		40 kN wheel load (section 412A4)		
		MDD4	MDD8	MDD12
80 kN wheel load (section 410A4)	MDD4	9.84	0.50	3.40
	MDD12	10.70	1.50	4.36
100 kN wheel load (section 410B4)	MDD4	7.44	0.37	2.57
	MDD12	8.16	1.11	3.31
	Average		***4.45***	
	Std Deviation		***3.70***	

6.7 CONCLUSIONS

The precracked phase of the emulsion treated material can be divided into two subphases, namely, the life to crack initiation and the effective fatigue life. The life to crack initiation is the phase before traffic induced cracking started in the layer and the layer is still intact with a relatively high stiffness. When microcracks start to develop at the bottom of the layer, these cracks will start to propagate through the layer. The material is then in a crack propagation phase. When the cracks have propagated through the layer, the stiffness of the layer is reduced to a value in the order of 500 MPa. The end of the effective fatigue life was defined to be when the layer reaches a stiffness of approximately 500 MPa. The layer will then behave similar to good quality granular material, although the layer is not physically in a granular state. Permanent deformation of the emulsion treated layer will then become the dominant failure mechanism. No definite value for the damage factor could be obtained and it is recommended that until further research develops more reliable values, a value of 4 should be used as normally used in pavement analysis (COLTO: 1996).

6.8 REFERENCES

ASTM, 1964, STP 91A: *Tentative guide for fatigue testing and the structural analysis of fatigue data*, 2nd edition, American Standard Test Methods, West Conshohocken, PA, Unites States.

Committee of Land Transportation Officials (COLTO), 1996, *Draft TRH4: Structural design of flexible pavements for interurban and rural roads*, Draft TRH4:1996, Department of Transport, Pretoria, South Africa.

Committee of Land Transportation Officials (COLTO), 1997, *Draft TRH12: Flexible pavement rehabilitation investigation and design*, Draft TRH12:1997, Department of Transport, Pretoria, South Africa.

De Beer M, 1989, Aspects of the design and behaviour of road structures incorporating lightly cemented layers, PhD Thesis, University of Pretoria, Pretoria.

Theyse HL, de Beer M, Prozzi J, Semmelink CJ, 1995, *TRH4 Revision (1995): Phase I: Updating the transfer functions for the South African Mechanistic Design Method*, NSC24/1, Department of Transport, Pretoria, South Africa.